Int J Adv Manuf Technol (2015) 78:1769–1780
DOI 10.1007/s00170-014-6777-4

ORIGINAL ARTICLE

Characterization of deformation behavior of thin-walled tubes during incremental forming: a study with selected examples

Tong Wen · Chen Yang · Suo Zhang · Lantao Liu

Received: 28 July 2014 / Accepted: 29 December 2014 / Published online: 15 January 2015

Abstract As an emerging flexible manufacturing technology, incremental forming of tubes has the ability to produce various tubular parts, including those that are difficult to integrally form using other methods. Due to the nature of hollow and thin-walled geometry, the deformation mechanism in the incremental forming of tubes is quite different from that of conventional incremental forming of sheets. This paper summarizes a list of typical tubing that can be formed incrementally and then examines the processes used to form four types of tubular parts, including axisymmetric expansion/reduction of tube ends, tube wall grooving, and hole flanging. This is done primarily from the perspective of phenomenology by using experiments and numerical simulation. Typical deformation behaviors of the workpieces were revealed and discussed. Three basic deformation modes in terms of variations in wall thickness, namely thinning (such as in end expansion), thickening (such as in end reduction), and invariant or almost constant thickness (such as in part of the wall grooving), were found to exist during incremental tube forming. Regarding the formability limits of the tube, incremental forming has its own advantages and disadvantages when compared with pressing.

Keywords Tubular part · Incremental forming · Flexible manufacturing · Deformation

T. Wen (✉) · C. Yang · S. Zhang · L. Liu
College of Materials Science and Engineering, Chongqing University, Chongqing 400044, China
e-mail: tonywen68@hotmail.com

1 Introduction

Metallic thin-walled tubular parts are widely used in the industrial environment as lightweight structural or distinctive functional components [1–3]. With the increasing demand for performance, function, and quality of modern products, tubular structures are becoming increasingly complex, inevitably leading to an awkward situation for traditional tube processing industries. Under the pressure of intensive global competition, the manufacturers in today's marketplace face many challenges to produce high-quality tubing in a cost-effective and productive way.

Flexible manufacturing that puts digital technology at the core is characterized by high agility and expansibility. It has attracted more and more attention in recent years due to the ability to meet diverse requirements of modern manufacturing. In the field of metal forming including tubing production, flexible manufacturing can play a significant role [4]. As a matter of fact, a couple of flexible or partially flexible tube-forming techniques have been developed during the previous decades, for instance, numerical control (NC) tube bending, NC tube-end forming, and NC laser cutting, amongst others [5–8].

Incremental forming is a flexible technology based on the principles of computer numerical control (CNC) machining and employing a method of so-called "layered manufacturing." During the process, formation of the complex 3D sheet metal parts is accomplished point by point according to CAD models, without the use of special tools or by using only simple ones. Thus far, this technology has mainly been applied in the forming of planar sheets, in particular, in production processes that include many varieties, in small and medium batches in the aerospace or automotive fields, and other similar areas [9–11]. A few attempts have also been made to produce tubular parts by using incremental forming technology. For example, Matsubara [12] examined a tube-nosing

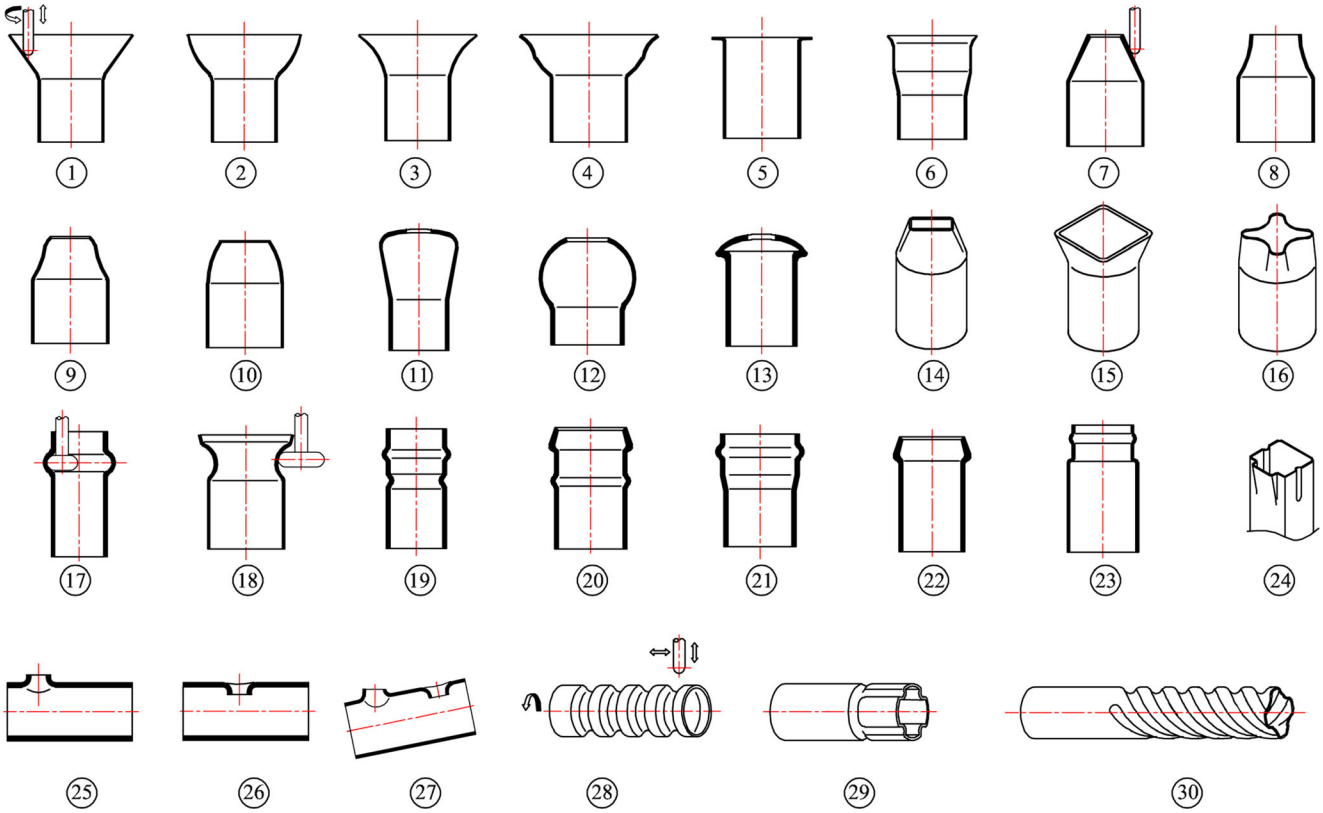

Fig. 1 Schematic illustration of tubular parts made by incremental forming

process in which a CNC-controlled forming tool was used to compress the open end of a tube into a variety of axisymmetric or polygonal forms; Teramae et al. [13] put forward an incremental burring process instead of welding for producing branched tubing. The authors [14] proposed a concept for fabricating some specially shaped tubular parts by incremental forming, including tubing with spiral grooves, which are difficult to form integrally using traditional approaches.

Despite a few differences, a combination of shear and stretching deformation that leads to wall thinning is the main deformation mechanism of the conventional incremental sheet forming. The relationship between the wall thickness (t) after forming, the wall angle (α), and the original wall thickness (t_0) usually obeys the *sine law* [15]

$$t_1 = t_0 \sin\alpha \tag{1}$$

In essence, dieless incremental tube forming is still a progressive deformation under the localized pressure of a bar tool; however, the force and deformation behavior are quite different from those in normal incremental sheet forming. Thus, the existing theoretical achievements of incremental forming are far from sufficient to guide the practice of incremental tube forming and there is a strong need for examining the fundamental deformation mechanics of the process.

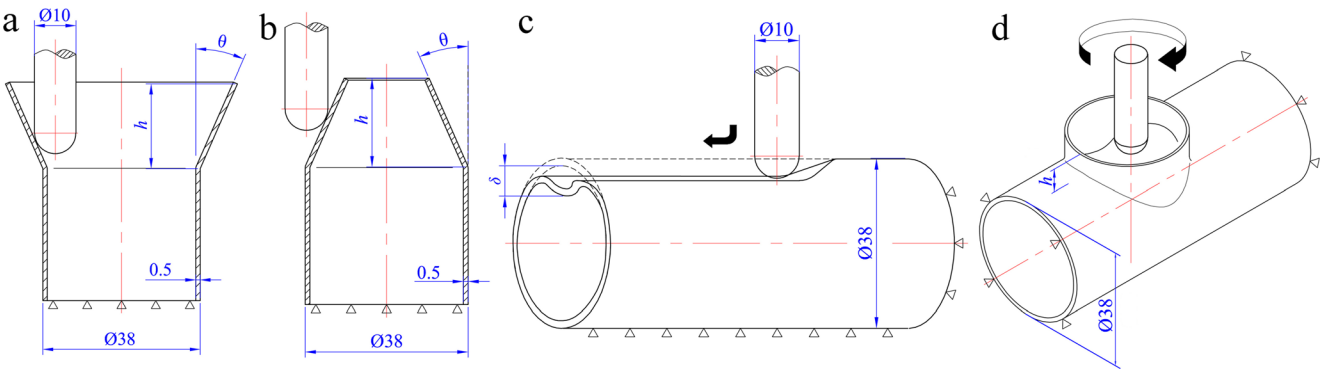

Fig. 2 Samples in the study. *Small triangles* represent constraint regions of the wall. **a** End expansion. **b** End reduction. **c** Grooving. **d** Hole flanging

The current work attempts to provide a new level of understanding for the incremental tube-forming technology, which has a potential application in practice. Typical tubular parts made using the technology were classified, and four types of processes including axisymmetric expansion/reduction of tube ends, grooving, and hole flanging on tube walls were selected as examples for investigating dieless incremental tube forming by experiment and numerical simulation. Characterization of the force and deformation behavior of thin-walled tubes during formation will be discussed, and key points of the technique will be addressed.

2 Outline of dieless incremental tube forming

As a flexible technology, in theory, incremental forming can produce a wide range of tubular parts and it can even handle profiles with open sections (which are not discussed in this paper). Based on existing studies [12, 13] and the authors' former work [14], typical tubular parts that could be formed by this approach are summarized and presented in Fig. 1. It is worth pointing out that tubing with various other geometries can also be made by combining these basic shapes.

2.1 End and localized forming

This includes axisymmetric or non-axisymmetric expansion and reduction of tube ends, and combined forming of end expansion and reduction, as shown in plots 1 to 16 in Fig. 1. Plots 14 to 16 are non-axisymmetric tube ends.

Localized forming consists of local bulging (beading) and depression, and tools with modified shapes can sometimes be utilized, as shown in plots 17 to 23. Plot 24 is a sample of localized forming on a noncircular tube.

Table 1 Mechanical properties of 316-L and Al 6061

			316 L	Al 6061
Density	ρ	kg/m^3	7980	2900
Young's modulus	E	GPa	195.0	68.9
Poisson's ratio	ν		0.3	0.4
Yield stress	σ_s	MPa	302.0	55.0

2.2 Hole flanging

There can be either inward or outward flanging of precut holes on a tube wall. The axis of the branching can be perpendicular or inclined to the axis of the mother tube, as shown in plots 25 to 27.

2.3 Wall grooving

There are straight and curved (or helical) grooves, as shown in plots 28 to 30. Formation of the curved grooves requires simultaneous motion of a tool and the mother tube. Rotation of the tube on its own axis can be carried out using an NC rotary table (or spiral head). Here, we will just consider straight grooves.

3 Analysis models

To represent different deformation modes, four types of dieless incremental tube-forming processes, i.e., expansion and reduction of the open end, tube wall grooving, and hole flanging, were selected as examples in the current study, as shown in Fig. 2.

For tube-end expansion/reduction, as shown in Fig. 2a, b, one end of the tube is fixed to the workbench, while another

Fig. 3 Photograph of the incremental forming machine

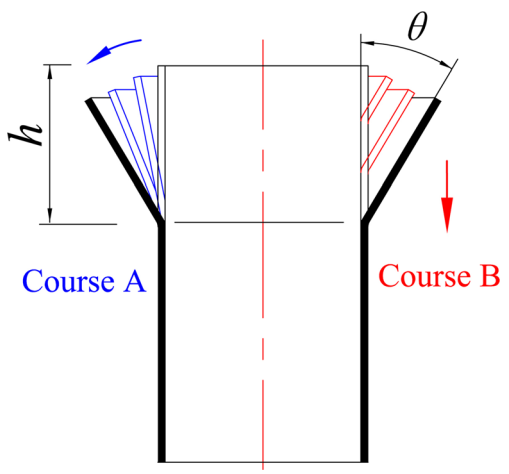

Fig. 4 Schematic of two processing courses

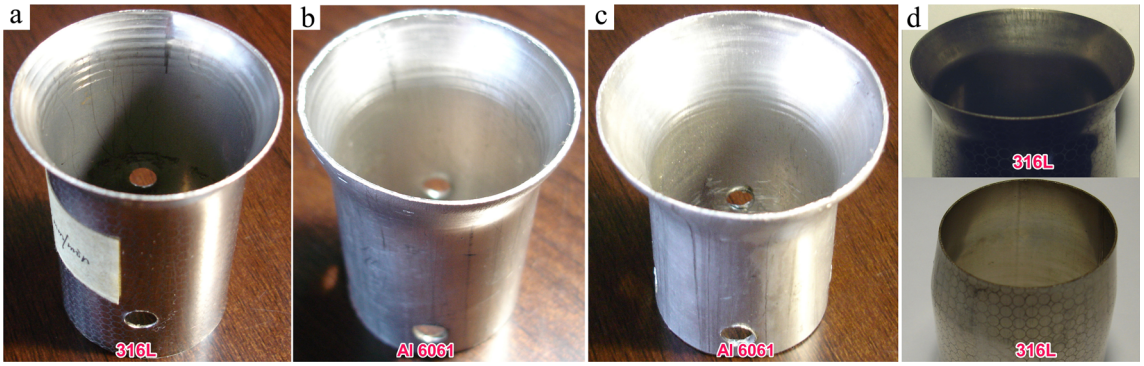

Fig. 5 Experiment results. **a**, **b** Incremental tube-end expansion, $\theta=10°$. **c** Incremental tube-end expansion, $\theta=30°$. **d** Tube-end expansion/reduction by pressing, $\theta=10°$

end of the tube is gradually formed to a desired shape with a bar tool.

For tube wall grooving, as shown in Fig. 2c, one end of the tube is fixed and the bottom is supported by a rigid plane. A bar tool then moves downwards and touches the extrados of the tube, denting the wall with different depths (δ), which were set to 2, 4, 6, 8, and 10 mm in the experiment; subsequently, the tool moves horizontally along the tube axis with a given distance, shaping a straight groove on the wall.

For hole flanging, as shown in Fig. 2d, after both ends of the tube were fixed with the precut hole facing upwards, the wall was progressively deformed under the pressure of a tool and then the branched tubing was formed. Circular branching with a flat edge is considered in this study.

The experiment was performed on an NH3525 incremental forming machine with maximum strokes of 250, 350, and 150 mm in the X, Y, and Z axes, respectively (see Fig. 3). Welded tubes made of 316-L stainless steel with a thickness of 0.5 mm and an outer diameter of 38 mm and seamless tubes made of 6061 aluminum alloy with a thickness of 1.0 mm and an outer diameter of 38 mm were used in the experiment. The mechanical properties of the materials were obtained from tensile tests carried out at room temperature, as presented in Table 1. The materials were assumed to be elastic-plastic. According to the tensile curves, the constitutive equations in the plastic domain are expressed as

$$\sigma = \sigma_s + B\varepsilon^n = 302 + 1002.4\varepsilon^{0.65}\ (\text{MPa}) \tag{2}$$

for 316 L, and

$$\sigma = \sigma_s + B\varepsilon^n = 55 + 738.2\varepsilon^{0.44}\ (\text{MPa}) \tag{3}$$

for Al 6061, where n is the strain-hardening exponent and B is the material constant.

The bar tool is made of Cr12MoV with a hardness of about 55 HRC after heat treatment. Preliminary tool paths employed in the experiment and the numerical simulation were generated in Unigraphics NX®. The tool was set to a constant speed of 250 mm/min. The finite element method (FEM) analysis was conducted in Abaqus®, where the 3D models were meshed with type S4R four-node shell elements. General machine oil was used as the lubricant. Interface friction was characterized by means of Coulomb's friction law, $\tau=\mu N$, and the friction coefficient μ was set to 0.2.

As with other incremental forming processes, tube wall deformation is markedly affected by the tool path. In an experimental study of spinning of a taper shape on the tube end, Yao et al. [16] employed two processing courses. In the

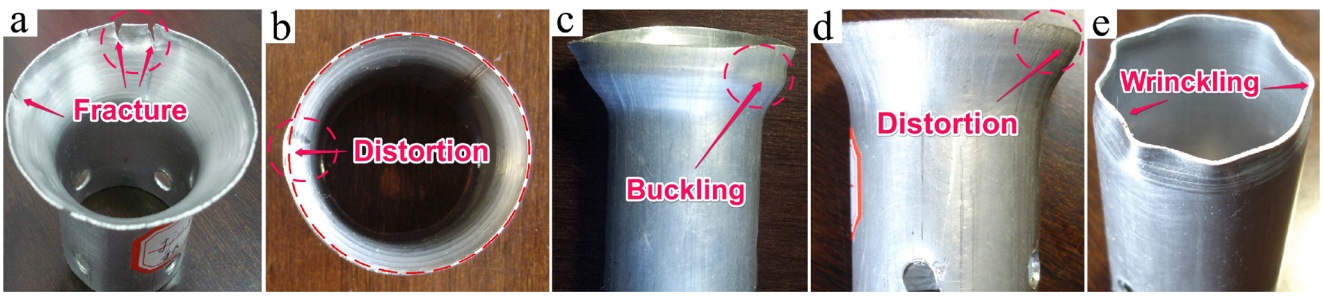

Fig. 6 Typical defects of incremental tube-end expansion/reduction of Al 6061 tubes. **a** Fracture. **b** Distortion of cross section. **c** Wall collapse. **d** Distortion of vertical section. **e** Wrinkling in reduction

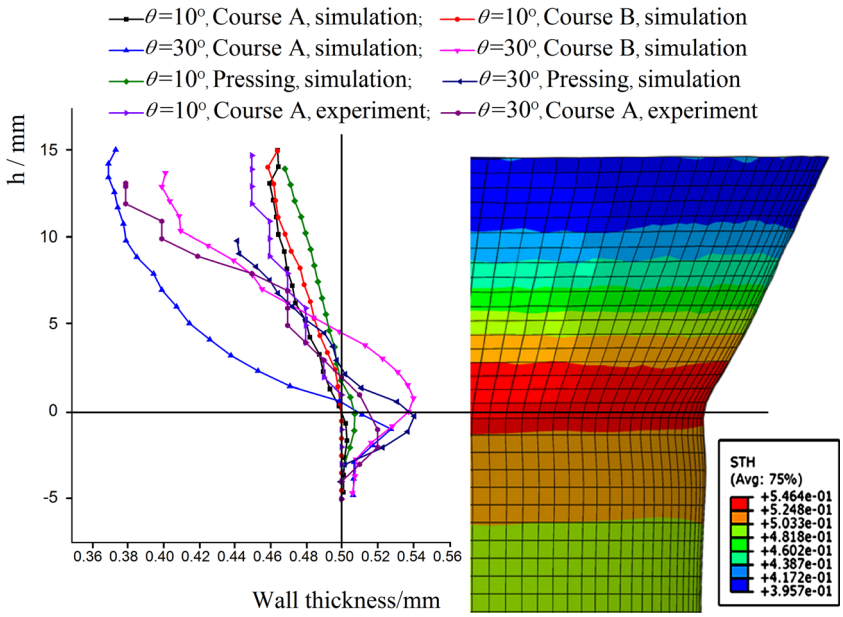

Fig. 7 Comparison of the wall thickness distribution of 316-L tube ends expanded using different methods

first one, the taper angle progressed gradually in the same forming region, while in the second course, the taper region progressed gradually with the same taper angle (θ). Accordingly, two similar processing courses for incremental end expansion and reduction, with equal forming length and equal taper angle (θ), were adopted in the study, as shown in Fig. 4. The angle (θ) was set to 10°, 30°, and 50° in the respective trials.

4 Results and observations

4.1 Incremental tube-end expansion and reduction

1. Basic deformation

Figure 5 shows the experimental results of tube-end expansion/reduction with varying taper angles (θ). The incremental forming processes were performed with the same bar tool, exhibiting the high flexibility and agility of the technique. Figure 6 shows the typical defects resulting from incremental forming, including fracture, distortion, wall collapse, wrinkling, and others. Processing lines can also be clearly observed on the surface of the incrementally formed wall. In the end expansions of the 316-L Al 6061 tubes with θ of 50°, formed by incremental forming and pressing, collapse occurred in both the experiment and the simulation.

Figure 7 compares the wall thickness distribution of 316-L tubes after incremental expansion with an original height (h) of 15 mm and different taper angles (θ). Results of end expansion by pressing on a conical die are also presented for comparison. It can be seen that, as a whole, wall thickness decreases gradually from the onset of expansion to the tube end, regardless of the forming methods and processing routes; in addition, wall thinning increases as the taper angle (θ) increases. When θ is small (such as 10°), the trend of the variation in wall thickness is almost linear. However, at the tube end, the thinning decreases slightly. This might be caused by a reduction in the height of the tube wall at the open end, where less constraint exists, and thus, the material can compensate. The deviation in the curve progression increases when θ is larger.

During the incremental tube-end expansion/reduction process, the tool undergoes a large dynamic

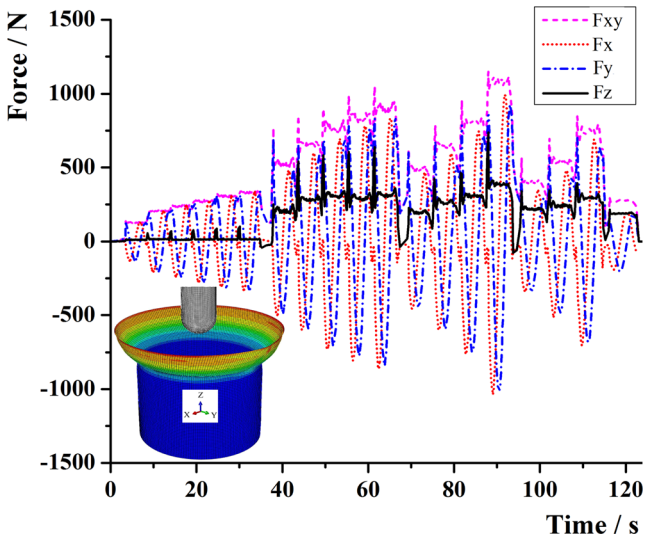

Fig. 8 Transient forces on the tool during incremental expansion of a 316-L tube end

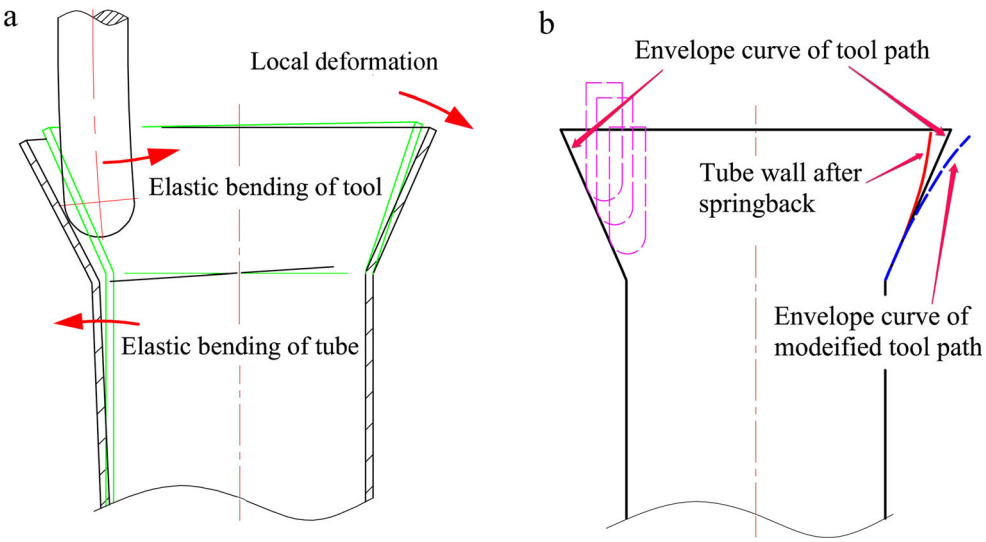

Fig. 9 **a** Elastic deformations and **b** tool path planning in the incremental expansion of the end

lateral force, since the side of the tool's hemispherical bottom is the main working zone. Figure 8 shows the simulated forces exerted on a tool during the whole expanding process with course A, i.e., forces along the *X*, *Y*, and *Z* axes, and the resultant force F_{xy} within the horizontal *X*-*Y* plane. It can be found that the forces F_x and F_y fluctuate in a way similar to sinusoidal waves, while the resultant lateral force F_{xy} remains almost constant within 1 cycle of the tool path around the tube axis. In contrast, the force F_z along the tool axis is smaller than F_{xy} during the entire process. The lateral force F_{xy} can be reduced by decreasing the feed pitch and optimizing the processing route.

Tube wall deformation is governed by stress conditions during the course of formation. It can be clearly seen that wall thickening occurs near the onset of expansion due to the downwards axial pressure from the tool during the incremental forming and pressing processes; meanwhile, we see that with course B, wall thickening within this region is larger than that with course A. If the axial force that is exerted on the tube is too large, the wall will buckle. Comparatively speaking, the axial force in incremental forming is smaller than that in pressing; thus, the trend of collapse or buckling is reduced. In the experiment, no collapse took place during the whole process of incremental 316-L tube expansion with θ of 10° and only slight collapse occurred when θ was 30°, whereas during pressing, axial collapse occurred at a stroke height of 14 mm with θ of 10° and at a stroke height of 10 mm with θ of 30°. Furthermore, when tube-end expansion (or

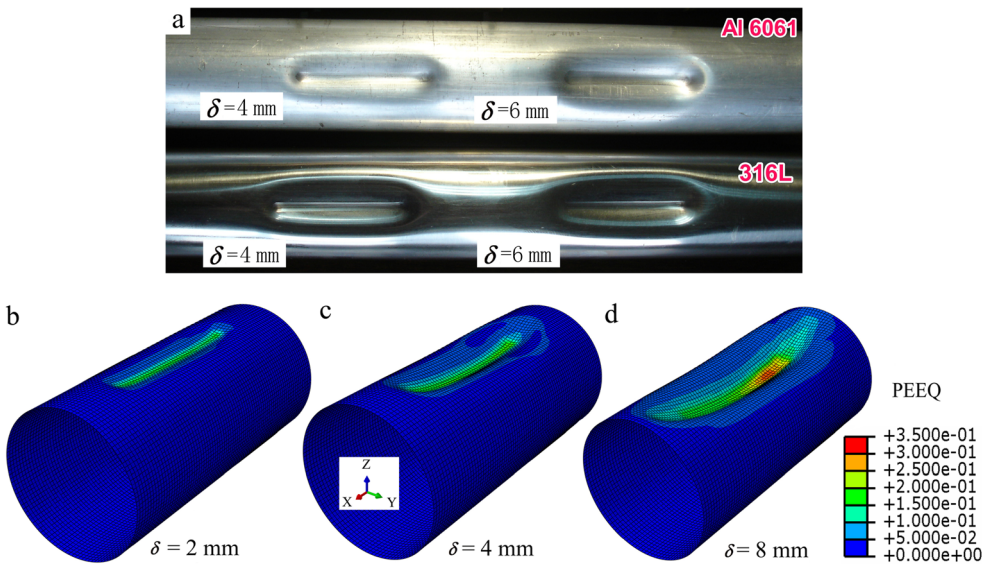

Fig. 10 **a**–**d** Experiment and simulation results of incremental tube grooving (316-L tubes were used in the simulation)

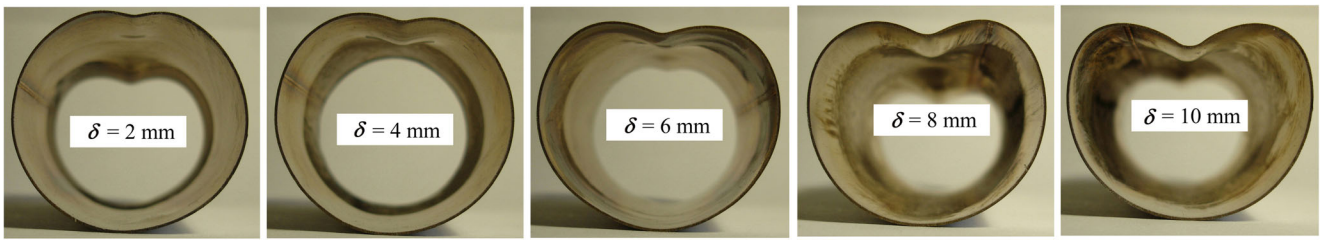

Fig. 11 Cross sections of incrementally grooved 316-L tubes

reduction) was conducted by pressing with a conical die, it was difficult to attain a large θ due to the so-called "folding effect" [17–19]. In other words, when the angle (θ) is too large, the open end will deform in a manner of inward or outward inversion under the axial pressure, rather than expansion or reduction.

Compressive hoop stress in tube-end reduction will lead to wall thickening and even wrinkling. It was found that wrinkling is more likely to occur in incremental reduction, because the stress distribution is nonuniform. In the experiment, end reduction by pressing with θ equal to 10° was successful, whereas wrinkling occurred in incremental forming, as shown in Fig. 6.

2. Elastic deformation and springback

Plastic deformation is always accompanied by elastic deformation; the latter brings about an undesired phenomenon such as consequent springback, which usually has a negative effect on the product, especially when forming a sheet metal at room temperature. Generally, in incremental tube-end expansion/reduction, the elastic deformations at varying degrees come from three aspects: the localized wall deformation, the overall elastic bending of the tube, and the elastic bending of the tool, as demonstrated in Fig. 9a. It is evident that the overall elastic tube bending increases with the distance between the deformation region and the location at which the tube is fixed.

Figure 9b shows the relationship between the envelope of the tool path during the final forming stage and the actual shape of the formed wall. Even though the envelope appears as a straight line from the side view, the section of the formed wall forms an arc. This is particularly notable when the feeding pitch is large (such as the 1 mm used in our experiment), since the localized wall rebound is largest at the open end. Thus, in order to obtain a straight section for the expanded wall, the springback compensation should be appropriately considered in the planning of the tool path and a smaller feeding pitch should be used.

4.2 Incremental tube wall grooving

1. Basic deformation

Tube wall grooving can be considered to be a static buckling and post-buckling process in which a thin cylindrical shell is centrally dented under concentrated external force. In some respects, it is similar to single-point incremental forming (SPIF) and the maximal forming load on the tool is the pressure along its axis. During the grooving, the tube wall is supported mostly by its own rigidity and the constraint on the wall is not as strong as it is on the sheet in incremental forming, where the outer periphery of the sheet is firmly clamped in a blank holder. Figure 10 shows some experimental and simulation results. When the groove is long enough along the axial direction, the in-plane deformations within the cross sections present the same mode; thus, it can be regarded as plane strain, except for the transitional sections close to the groove ends.

Figure 11 shows the cross sections of 316-L tubes grooved with varying dent depths in the

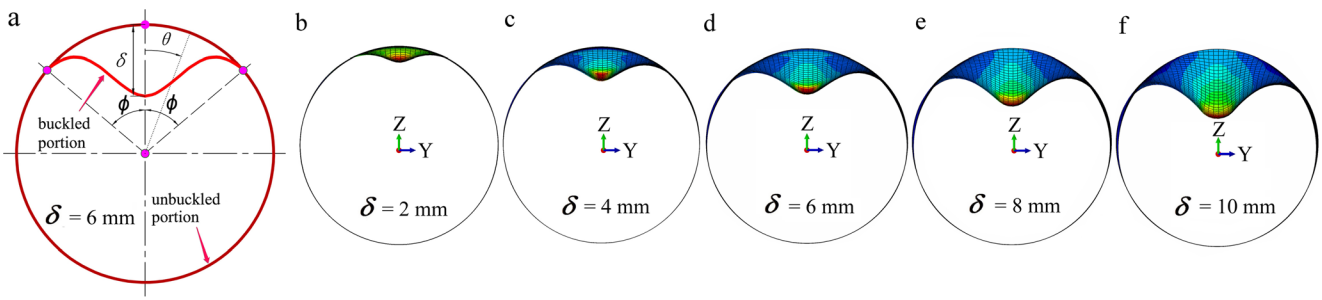

Fig. 12 Comparison of cross sections. **a** Schematic representation of Glock's model. **b–f** FEM results of 316-L tubes

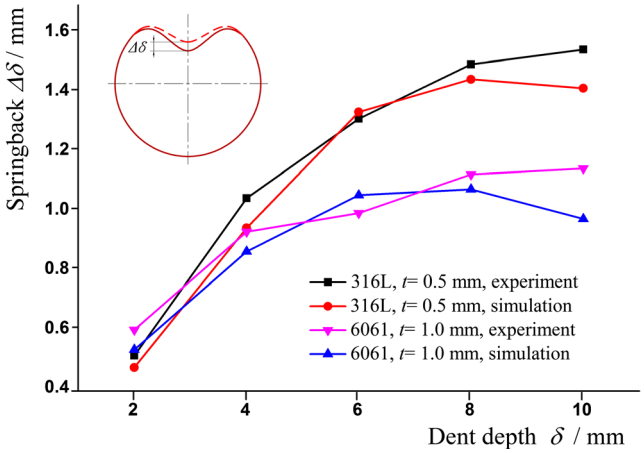

Fig. 13 Springback vs. δ. The data were measured at the centers of the grooves, with lengths of 40 mm

experiment. It should be noted that due to significant elastic recovery after unloading, the actual dent depths are smaller than the designed values.

With an assumption that an elastic cylindrical shell subjected to external pressure will buckle, the dent shapes have been studied by several researchers with the purpose of determining the effect of dent on the critical buckling axial pressure of thin shell structures [20, 21], where the dent was considered as a geometrical imperfection. For instance, Rathinam et al. [20] gave an equation for modeling the dent shape as follows:

$$\rho = \frac{1}{4}\left[\left\{1+\cos\left(\frac{2\pi x_1}{L}\right)\right\}\left\{1+\cos\left(\frac{2\pi x_2}{W}\right)\right\}\right] \quad (4)$$

where ρ is the radial inward displacement of the dent; L and W are the length and width of the dent, respectively; x_1 is the distance from the center of the dent to the point on the longitudinal axis of the dent with

$$-L/2 < x_1 < L/2 \text{ and} -W/2 < x_2 < W/2 \quad (5)$$

and x_2 is the distance from the center of the dent to the point on the transverse axis of the dent.

Glock [21] presented a solution for external pressure buckling of elastic rings confined within a rigid medium. As shown in Fig. 12a, ring deformation consists of two parts: the buckled portion and the unbuckled portion. An assumed shape function $w(\theta)$ for the buckled region was deduced as follows:

$$w(\theta) = \delta\cos^2\left(\frac{\pi\theta}{2\phi}\right) \quad (6)$$

where $w(\theta)$ is the tangential displacement of the ring reference line at mid-thickness, Φ is the angle that defines the border between the buckled and the unbuckled ring portions, and $-\Phi \le \theta \le \Phi$.

The configuration of the deformed tube section within the buckled region in Fig. 12a was depicted according to Eq. (6). It can be found that the analytical result is consistent with the numerical simulation, as presented in Fig. 12d. Nevertheless, due to the loose constraint on the tube, we can observe a slight collapse of the wall, which distorts the roundness of the cross section, especially when the dent is deep.

From formulas (4) and (6), we see that the shape of the cross section has little to do with the properties of the material; in other words, mechanical parameters such as stiffness and strength have little effect on the shape of the cross section during the buckling stage. It should be mentioned that this conclusion neglects the effects of springback and the plastic deformation.

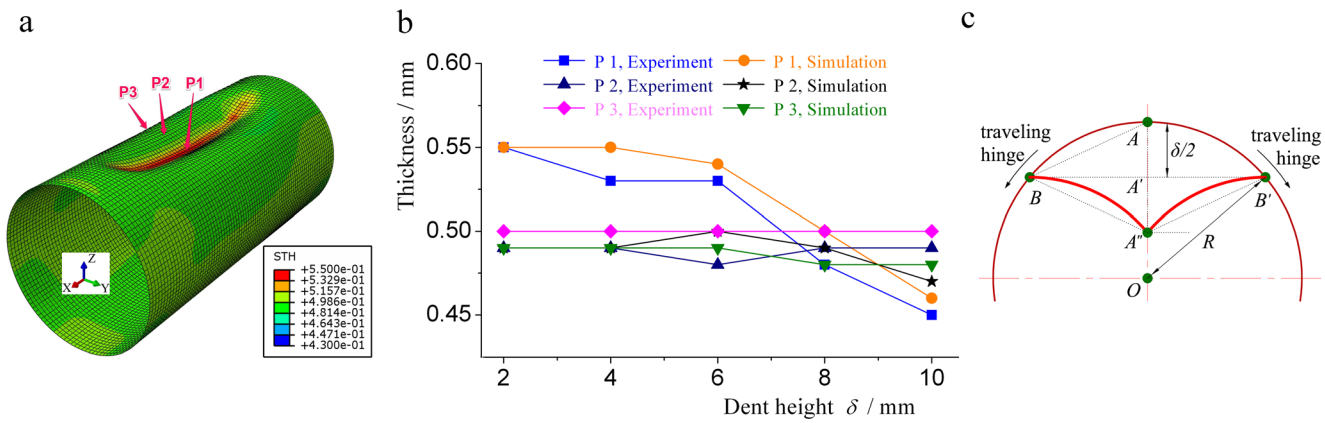

Fig. 14 Thickness variation and the three-hinge model. **a** Thickness distribution of the 316-L tube, with a dent depth (δ) of 4 mm. **b** Thickness vs. δ. **c** Definition of the model

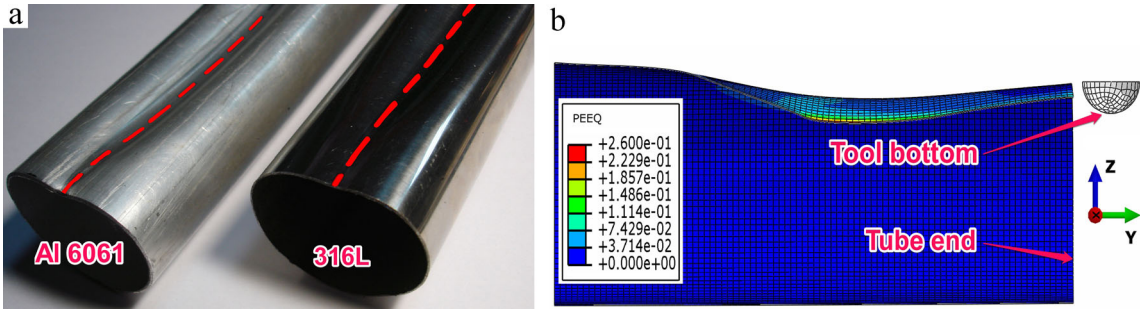

Fig. 15 End effect in incremental tube grooving. **a** Experimental samples, δ=6 mm. **b** Numerical result, 316-L tube after springback

Figure 13 shows the relationship between the springback and the dent depth (δ). It can be found that the springback of the 316-L tubes is larger than that of the Al 6061 tubes, due to a higher ratio of yield strength to Young's modulus and thinner relative thickness [22], indicating that the material properties and workpiece geometry have a significant influence on the springback. The increase in the springback slows down after the dent depth reaches about 6 mm.

2. Thickness variation

It is known that when forming a dent on a wide plate by using pressure (for example, embossing a bead on sheet metal), the plate bulges locally and the bottom thins. The degree to which the wall thins increases with the depth of the dent, and it decreases with the reduction of the plate width, due to the compensation of material flowing from the surrounding region, presenting a deformation mode similar to that in deep drawing. Figure 14a, b shows the variation in thickness of incrementally grooved tubes at three points P1, P2, and P3 within the buckled portion. It can be seen that the overall change in the thickness of the wall is small; however, the bottom of the groove (P1) is slightly thicker than the original thickness of 0.5 mm; meanwhile, the amount of thickening at P1 decreases with increasing dent depth.

This phenomenon can be understood with the three-hinge model developed by Vasilikis et al. [20], as shown in Fig. 14c. The model uses an approximation of the plastic-hinge mechanism to illustrate the post-buckling collapse behavior of a confined cylinder, subjected to external pressure. It is symmetric with respect to the θ= 0 axis, with two moving plastic hinges at B and B' and one stationary plastic hinge initially located at A.

When the convex wall begins to collapse inwards under the pressure of the tool, with the downward movement of joint A, the length of the arc BAB' is shortened and the hoop stress within the wall is compressive, resulting in thickening of the wall. Theoretically, arc BAB' reaches its shortest length when joint A touches line $\overline{BB'}$, that is, when A reaches A'. After that, as the collapse continues, the hoop stress turns to tensile force, gradually leading to thinning of the wall.

As shown in Fig. 14b, at P1, the wall thickens first, but the degree of thickening continuously decreases with δ; when δ reaches about 8 mm, the wall begins to thin. It should be noted that since the constraint on the tube wall is limited during this process, a condition of approximately free deformation exists. One phenomenon is that as δ increases, first the compressive and then the tensile hoop stresses push and pull the wall on both sides of the groove, eventually leading to inward curling of the wall. The traveling hinges BB' move down, and the trend of wall thinning at the groove bottom is alleviated. Therefore, the overall variation in wall thickness during the whole

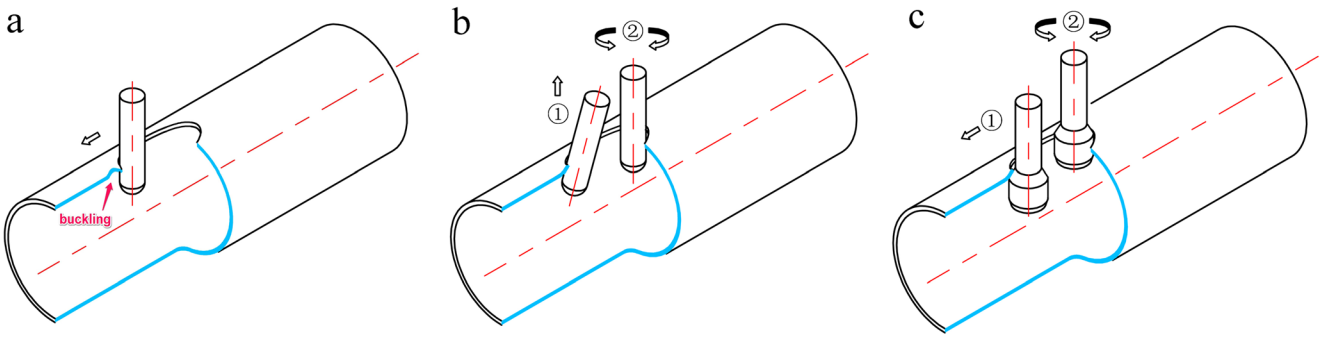

Fig. 16 **a**–**c** Principle of dieless incremental hole flanging on thin-walled tubes under different tool states

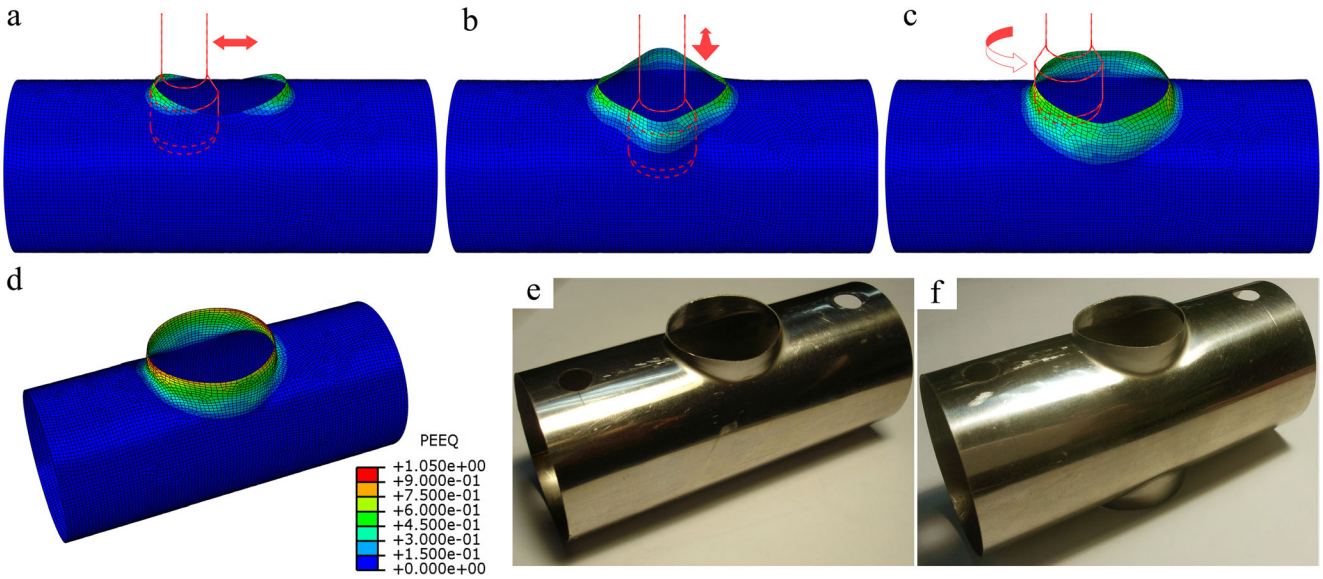

Fig. 17 Incremental hole flanging of the 316-L tube. **a**, **b** Preforming. **c** Shaping. **d** After forming. **e** Experiment specimen, tee fitting. **f** Experiment specimen, cross fitting

process is restricted to less than about 10 % in our study. Under these circumstances, fractures may not be the primary mode of failure.

3. End effect

In the bending of a tube, bending too close to the ends will cause it to distort and be drawn out of square from the side view; thus, the end plane will no longer be perpendicular to the tube axis [23]. This phenomenon, which is relevant to variations in the load state and the distribution of stress near the tube ends during the formation process, is sometimes called the end effect [24, 25]. The effect was also observed in tube wall grooving, in which the ends of the tube did not deform as much as the mid-sections, even with the same denting depth. This resulted in curvature changes near the end of the shell structures, as shown in Fig. 15. At the dented end, the 316-L tubes were found to have larger springback than did the Al 6061 tubes.

4.3 Incremental hole flanging on the tube wall

When a traditional columnar tool is used for the incremental hole flanging on a tube, at the beginning, the force that the tool exerts on the rim of a precut hole at the extrados is nearly parallel to the tube wall along the tube axis, as shown in Fig. 16a. Under this condition, the initial curling direction of the hole rim is random and the wall could bend downwards, resulting in failure. Teramae et al. [13] introduced a preforming stage to wedge the wall up with the tool held obliquely, as shown in Fig. 16b. After that, the inclined wall can be flanged to the desired shape and dimension; however, it is necessary to rotate the axis of the tool from the vertical. The authors put forward a modified tool with a tapered shoulder, as shown in Fig. 16c, with which the incremental hole flanging can be performed without changing the orientation of the tool from vertical. Here, we are primarily concerned with the basic deformation behavior of the tube; detailed conclusions regarding the effect of the processing parameters, such as tool shape

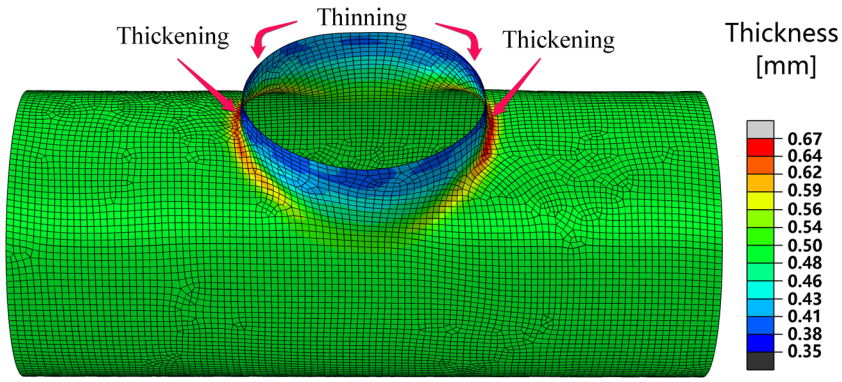

Fig. 18 Thickness distribution of the 316-L tube after incremental hole flanging

and path, on the wall deformation will be discussed separately [26].

Figure 17 shows the numerical and experimental results of incremental hole flanging on a 316-L tube, using the improved tool. For a circular branch, the precut hole on the mother tube was oval rather than circle from the vertical view because of the cambered wall shape. In our study, the bar tool moved horizontally along the direction of the tube axis and then applied an upward curl to the rims of the precut holes on both sides (the major axis of the oval hole) with the inclined surface of the tool; then, the hole was flanged along its minor axis (perpendicular to the tube axis), as shown in Fig. 17a, b. Subsequently, the bar tool moved around the hole several times, gradually flanging the wall until the desired shape was attained. Tube fitting with double sides (cross) or more branching can also be made using this method.

Figure 18 shows the simulated thickness distribution after flanging; the theoretical result is in very good agreement with the experimental result [26]. Near the branch edge, the wall is obviously thinned, and if the branch is too high or the diameter is too large, a fracture would take place at the edge due to the excessive thinning of the wall. A fracture is also likely to occur if there are burrs on the rim of the precut hole; thus, the initial hole edge should be polished smoothly in order to improve the formability of the material. Unlike flanging a hole on a plate by pressing or by incremental forming [27], wall thickening, which was caused by horizontal pressure from the tool, was observed at both sides of the branch root along the axial direction. Certainly, thickening within this transition region is a benefit of promoting the stiffness and strength of the tubular structure. Nevertheless, buckling would occur if the horizontal pressure, i.e., the reacting force of the lateral force exerted on the tool, is too large.

5 Conclusion

1. Although incremental tube forming is a progressive process under localized pressure, the force and deformation mode are different from those found in conventional incremental sheet forming. There are three wall deformation modes: thinning, thickening, and invariant thickness. For a specific type of tubing, the actual wall deformation will be a combination of these basic modes.
2. Elastic deformations make up a relatively large proportion of the total deformations of the tube, and so, the corresponding springback is significant. Possible defects include fractures, distortions, wrinkling, collapse, buckling, and processing lines. Regarding the formability limits of tube, incremental forming and pressing with a die each have their own advantages and disadvantages, since the failure representations of the tube are varying.
3. Tube wall deformation is affected by many factors, including workpiece geometry, processing parameters, and material properties. Besides the key points necessary for conventional incremental sheet forming, incremental tube forming requires additional considerations, such as the shape of the tool and how the tube is fixed in place. To guarantee an overall quality, it is essential to select reasonable values of the processing parameters and to achieve a compatible deformation of the wall during the process.
4. Modified bar tools can be used in some incremental tube-forming processes. The nontraditional tools would bring about a different way of applying force and deforming the walls.

Acknowledgments The work was supported by National Key Technologies R&D Program of China (2012ZX04010-081).

References

1. Green DE, Angara TS, Nurcheshmeh M, Wormald T (2012) A practical method to evaluate the forming severity of tubular hydroformed parts. Int J Adv Manuf Technol 62(9–12):965–980
2. Hashmi MSJ (2006) Aspects of tube and pipe manufacturing processes: meter to nanometer diameter. J Mater Process Tech 179:5–10
3. Tabatabaei SA, Shariat PM, Mosavi MM, Tabatabee SM, Aghajanzadeh M (2013) Optimum design of preform geometry and forming pressure in tube hydroforming using the equi-potential lines method. Int J Adv Manuf Technol 69(9–12):2787–2792
4. Allwood JM, Utsunomiya H (2006) A survey of flexible forming processes in Japan. Int J Mach Tool Manu 46(15):1939–1960
5. Alves LM, Dias EJ, Martins PAF (2011) Joining sheet panels to thin-walled tubular profiles by tube end forming. J Clean Prod 19(6–7): 712–719
6. Yang H, Li H, Zhang ZY, Zhan M, Liu J, Li GJ (2012) Advances and trends on tube bending forming technologies. Chinese J Aeronaut 25(1):1–12
7. Wen T (2014) On a new concept of rotary draw bend-die adaptable for bending tubes with multiple outer diameters under non-mandrel condition. J Mater Process Tech 214(2):311–317
8. Hsieh HS, Lin J (2005) Study of the buckling mechanism in laser tube forming with axial preloads. Int J Mach Tool Manu 45(12–13): 1368–1374
9. Emmens WC, Sebastiani G, Boogaard AH (2010) The technology of incremental sheet forming—a brief review of the history. J Mater Process Tech 210(8):981–997
10. Zhang C, Xiao HF, Yu DH (2013) Incremental forming path-generated method based on the intermediate models of bulging simulation. Int J Adv Manuf Technol 67(9–12):2837–2844
11. Ambrogio G, Filice L, Gagliardi F (2012) Improving industrial suitability of incremental sheet forming process. Int J Adv Manuf Technol 58(9–12):941–947
12. Matsubara S (1994) Incremental nosing of a circular tube with a hemispherical head tool. J JSTP 35:256–261
13. Teramae T, Manabe K, Ueno K, Nakamura K, Takeda H (2007) Effect of material properties on deformation behavior in incremental tube-burring process using a bar tool. J Mater Process Tech 191(1–3): 24–29

14. Wen T, Yang C, Chen X (2013) A method for producing special-shaped tubular parts based on dieless NC incremental forming process. Chinese patent, 201310005922.7
15. Jackson K, Allwood JM (2009) The mechanics of incremental sheet forming. J Mater Process Tech 209(3):1158–1174
16. Yao J, Murata M (2005) An experimental study on spinning of taper shape on tube end. J Mater Process Tech 166(3):405–410
17. Almeida BPP, Alves LM, Rosa PAR, Brito AG, Martins PAF (2006) Expansion and reduction of thin-walled tubes using a die: experimental and theoretical investigation. Int J Mach Tool Manu 46(12–13):1643–1652
18. Lu YH (2003) Study of tube flaring ratio and strain rate in the tube flaring process. Finite Elem Anal Des 40(3):305–318
19. Leu DK (2000) The curling characteristics of static inside-out inversion of metal tubes. Int J Mach Tool Manu 40(1):65–80
20. Rathinam N, Prabu B (2013) Static buckling analysis of thin cylindrical shell with centrally located dent under uniform lateral pressure. Int J Steel Struct 13(3):509–518
21. Vasilikis D, Karamanos SA (2009) Stability of confined thin-walled steel cylinders under external pressure. Int J Mech Sci 51(1):21–32
22. Li H, Yang H, Song FF, Zhan M, Li GJ (2012) Springback characterization and behaviors of high-strength Ti–3Al–2.5V tube in cold rotary draw bending. J Mater Process Tech 212(9):1973–1987
23. Miller G (2003) Tube forming processes: a comprehensive guide. SME, Dearborn
24. Orynyak IV, Radchenko SA (2007) Analytical and numerical solution for a elastic pipe bend at in-plane bending with consideration for the end effect. Int J Solids Struct 44(5):1488–1510
25. Moshksar MM, Borji S (1994) End effect in the explosive forming of tubes. J Mater Process Tech 42(4):431–441
26. Yang C, Wen T, Liu LT, Zhang S, Wang H (2014) Dieless incremental hole-flanging of thin-walled tube for producing branched tubing. J Mater Process Tech 214(11):2461–2467
27. Centeno G, Silva MB, Cristino VAM, Vallellano C, Martins PAF (2012) Hole-flanging by incremental sheet forming. Int J Mach Tool Manu 59:46–54